ResearchGate

See discussions, stats, and author profiles for this publication at: https://www.researchgate.net/publication/264680675

Nonisothermal crystallization kinetics of linear metallocene polyethylenes

ARTICLE *in* JOURNAL OF APPLIED POLYMER SCIENCE · MARCH 2008

Impact Factor: 1.77 · DOI: 10.1002/app.27392

CITATIONS
14

READS
10

1 AUTHOR:

Ibnelwaleed A Hussein

King Fahd University of Petroleum and Minerals

126 PUBLICATIONS **910** CITATIONS

SEE PROFILE

Available from: Ibnelwaleed A Hussein
Retrieved on: 27 January 2016

Nonisothermal Crystallization Kinetics of Linear Metallocene Polyethylenes

Ibnelwaleed A. Hussein

Department of Chemical Engineering, King Fahd University of Petroleum & Minerals, Dhahran 31261, Saudi Arabia

Received 18 June 2006; accepted 26 June 2007
DOI 10.1002/app.27392
Published online 19 November 2007 in Wiley InterScience (www.interscience.wiley.com).

ABSTRACT: The effect of weight-average molecular weight (M_w) on the nonisothermal crystallization kinetics of linear metallocene polyethylene (m-PE) was studied with modulated differential scanning calorimetry. Six linear m-PEs of molecular weights in the range 122–934 kg/mol were prepared by gas-phase polymerization. The cooling rate (R) was varied in the range 2–20°C/min, and it significantly affected the crystallization behavior. M_w had a weak influence on both the peak crystallization temperature and the crystallization onset temperature. All m-PEs showed primary and secondary crystallizations. At both low and high R's, the crystallinity showed a significant drop ($\sim$ 30%) when M_w was increased from 122 to 934 kg/mol. At low R's (< 10°C/min), the rate parameters in the modified Avrami method [primary rate constant (k_R)] and Mo method [$F(T)$] of analyses agreed in suggesting that an increased M_w slowed the rate of crystallization. The M_w dependency of k_R followed the Arrhenius type ($k_R = k_{Ro}e^{281}/M_w$, where k_{Ro} is a rate-dependent constant). However, at higher R's, k_R approached a constant value. The order parameters obtained by the different methods of analysis (n and α) were independent of M_w, which suggests that the crystal type remained the same. Hoffman–Lauritzen theory was used for data analysis, and activation energy per segment showed a significant decrease, from 225.0 to 11.8 kJ/mol, when M_w was increased from 152 to 934 kg/mol. Finally, all methods of analysis suggested a significant effect of M_w on slowing the overall crystallization process. © 2007 Wiley Periodicals, Inc. J Appl Polym Sci 107: 2802–2809, 2008

Key words: calorimetry; crystallization; kinetics (polym.); metallocene catalysts; polyethylene (PE)

INTRODUCTION

The investigation of the melting and crystallization behaviors of polymers is influenced by molecular structure. The study of polymer crystallization kinetics is important from theoretical and practical points of view,[1–5] and many researchers have studied the crystallization behavior of different polyethylenes.[6–11] The influence of molecular structure and crystallization conditions on the crystallization behavior of ethylene/α-olefin copolymers have been studied.[12–25] Most of these studies have used Ziegler–Natta polyethylenes (ZN-PEs), which are known for their heterogeneity in size and composition.[12,14,17,21,26] Also, the previous studies have primarily used fractions of conventional heterogeneous ZN-PEs. Hence, the effect of individual structural parameters on the crystallization phenomenon was difficult to separate. Metallocene polyethylenes (m-PEs) have narrow molecular weight distributions (MWDs) in the range 2–3, and for linear ZN-PE, MWD is the only interfering parameter.

Several studies on the thermal properties and molecular structure of polyethylenes (PEs) have been reported by different authors.[22,25,27–37] Most of these studies have used linear low-density polyethylene with a focus on the influence of short-chain branch distribution on the melting and crystallization kinetics,[22,27–29,33,36,37] particularly of a single polymer and its fractions with different fractionation techniques.[31,32,34–36] Modulated differential scanning calorimetry (MDSC) has been the main technique used to study melting and crystallization kinetics. However, the influence of weight-average molecular weight (M_w) on the nonisothermal crystallization kinetics of linear m-PEs has yet to be studied. I feel that the main reason behind that is the difficulty of finding commercial linear m-PE with different M_w's. So, in this study experimental resins were prepared to investigate the influence of M_w on the nonisothermal crystallization kinetics of linear m-PE with MDSC.

EXPERIMENTAL

Materials and sample preparation

Six linear PE samples were prepared by gas-phase polymerization. Laboratory-prepared catalysts were

Correspondence to: I. A. Hussein (ihussein@kfupm.edu.sa).

Contract grant sponsor: King Abdul Aziz City for Science and Technology; contract grant number: AT-22-16.

© 2007 Wiley Periodicals, Inc.
WILEY InterScience® DISCOVER SOMETHING GREAT

TABLE I
Characterization of the Linear m-PEs

Resin	Ethylene added (psi)	Hydrogen added	Temperature (°C)	M_w (kg/mol)	M_w/M_n
M122	200	Yes	80	121.8	2.34
M155	200	Yes	70	155.1	2.07
M160	200	No	60	160.0	2.35
M169	200	No	60	169.4	2.17
M172	200	No	80	171.6	2.12
M934	100	No	50	934	2.86
Standard				49.6	2.95

M_n = number-average molecular weight.

used for all of the PE syntheses. For samples M122–M172, $(n\text{-BuCp})_2$ $ZrCl_2$ on a polymeric support treated with methyl aluminoxane was used. A proprietary nonmetallocene catalyst was used for the synthesis of sample M934. The number associated with each sample is the M_w of that sample (see Table I). GPC results for sample M934 were not reliable because it was difficult to dissolve the sample, and heating to 170°C was required; this resulted in sample deterioration. The columns used were also not well suited for analyzing samples with M_w's as high as those of sample M934. The true M_w of this sample was very likely over 1,000,000, and the polydispersity was probably close to 2.5, as suggested by S. E. Wanke of the University of Alberta. The molar mass measurements were done with an Alliance GPCV 2000 instrument from Waters (Edmonton, Alberta, Canada), equipped with three HT6E columns. Trichlorobenzene was used as the solvent, and Millennium software from Waters was used to process the data. The standard had a M_w of 53 kg/mol and a polydispersity of 2.9. The synthesis and molar mass characterization of the samples were done in Wanke's laboratory. Before differential scanning calorimetry testing, all powder samples were melt-blended at our laboratory in a Haake melt blender at 190°C and 50 rpm for 10 min in the presence of 3000 ppm extra antioxidant. The main reason for the addition of the antioxidant was to save the polymer from degradation during testing.[38]

MDSC

MDSC measurements were performed with a TA Q1000 instrument equipped with a liquid nitrogen cooling system and an autosampler. Nitrogen at a flow rate of 50 mL/min was used to purge the instrument. Polymer samples (7.5–9.8 mg) were sliced and compressed into nonhermetic aluminum pans. To minimize the thermal lag between the sample and the pan, samples with flat surfaces were used. An empty aluminum pan was used as a reference. I removed the previous thermal effects by heating the samples to 140°C and holding them at this temperature for 5 min. All of the samples were cooled to subambient temperatures for complete evaluation of crystallization.[21] The samples were cooled from 140 to 5°C at a rate of 2°C/min (with ±0.2°C modulation), 4°C/min (with ±0.4°C modulation), and 6°C/min (with ±0.6°C modulation) every 40 s. First, the baseline was calibrated with empty crimped aluminum pans. The melting temperature and heat of fusion were calibrated with a high-purity Indium standard (156.6°C and 28.45 J/g). A sapphire disc was used to measure heat capacity. The absolute crystallinity (X_c) was calculated with the heat of fusion of a perfect polyethylene crystal, 290 J/g (see ref. 39, p 347). Here, the reversing and nonreversing heat capacity approach[40] was used for data analysis. Data of the nonreversing curve was processed with Universal analysis software (provided by TA Instruments, Inc.) to obtain the crystallization parameters.

Nonisothermal crystallization kinetics

Several analytical methods have been developed to describe the nonisothermal crystallization kinetics of polymers: (1) modified Avrami analysis,[1,41–43] (2) Ozawa analysis,[1] (3) Ziabicki analysis,[44,45] and other methods.[46,47] In this study, the modified Avrami analysis proposed by Jeziorny[2] and the Mo method suggested by Liu et al.[48] were used to describe the nonisothermal crystallization kinetics of m-LLDPEs. Because of the variation in the range of crystallization temperatures, the Ozawa model[1] was not suitable for this study. The Avrami equation is defined as follows:[41–43]

$$1 - X_t = \exp(-k_t t^n) \quad (1)$$

where n is the Avrami crystallization exponent, which is dependent on the nucleation mechanism and growth dimensions; t is the crystallization time; k_t is the growth rate constant, which depends on

nucleation and crystal growth; and X_t is the relative crystallinity.[43] X_t is defined as follows:

$$X_t = \frac{\int_{t_o}^{t}(dH_c/dt)dt}{\int_{t_o}^{t_\infty}(dH_c/dt)dt} \quad (2)$$

where dH_c/dt is the rate of heat evolution and t_o and t_∞ are the onset and completion times of the crystallization process, respectively. The Avrami equation was developed on the basis of the assumption that the crystallization temperature is constant. Jeziorny[2] modified the equation to describe nonisothermal crystallization. At a chosen cooling rate (R), the relative crystallinity is a function of the crystallization temperature (T). That is, eq. (2) can be formulated as

$$X_T = \frac{\int_{T_o}^{T_c}(dH_c/dT)dT}{\int_{T_o}^{T_\infty}(dH_c/dT)dT} \quad (3)$$

where X_T is the relative crystallinity as a function of crystallization temperature, T_o denotes the crystallization onset temperature, and T_c and T_∞ represent the crystallization temperatures at time t and after the completion of the crystallization process, respectively. t can be converted from T_c with the following equation[1,45] (which is strictly valid when the sample experiences the same thermal history):

$$t = \frac{T_o - T}{R} \quad (4)$$

where R is the cooling rate (°C/min). The double-logarithmic form of eq. (1) yields

$$\ln[-\ln[1 - X_t]] = \ln k_t + n\ln t \quad (5)$$

Thus, n and the crystallization rate constant (k_t) can be obtained from the slope and intercept of the plot of $\ln[-\ln(1 - X_c)]$ versus $\ln t$, respectively, for each R. The physical meaning of k_t and n cannot be related to the nonisothermal case in a simple way; they provide further insight into the kinetics of nonisothermal crystallization. The rate of nonisothermal crystallization depends on R. Therefore, k_t can be corrected to obtain the corresponding primary rate constant (k_R) at a unit R[1]:

$$\ln k_R = \ln k_t / R \quad (6)$$

A method modified by Mo, which combines the Avrami equation with the Ozawa equation, was also used to describe the nonisothermal crystallization. Its final form is given next:[48]

$$\ln R = \ln F(T) - \alpha \ln t \quad (7)$$

where Mo modified crystallization rate parameter ($F(T)$) $= [k(T)/k_t]^{1/m}$ represents the value of R and α is the ratio of n to the Ozawa exponent (m; $\alpha = n/m$).

Furthermore, the effective activation energy (ΔE_x) was calculated theoretically with the method proposed by Vyazovkin and Sbirrazzuoli.[49] In this method, the coefficient of the growth rate (G) and the overall crystallization rate (dX/dt) are related by

$$-E/R = \frac{d\ln G}{dT^{-1}} = \frac{d\ln(dX/dt)}{dT^{-1}} \quad (8)$$

G is given as a function of T_c by the Hoffman–Lauritzen equation in the context of the Hoffman–Lauritzen secondary nucleation theory.[50] Vyazovkin and Sbirrazzuoli[49] modified the Hoffman–Lauritzen equation to calculate ΔE_x at a given conversion (X) from the following relationship:

$$\Delta E_x = U^* \frac{T^2}{(T - T_\infty)^2} + K_g R \frac{(T_m^o)^2 - T^2 - T_m^o T}{(T_m^o - T)^2 T} \quad (9)$$

where U^* denotes the activation energy per segment, which characterizes the molecular diffusion across the interfacial boundary between melt and crystals; T_∞ is usually set equal to $T_g - 30$ K, where T_g is the glass-transition temperature of the polymer; K_g is a nucleation constant; T_m^o is the equilibrium melting point for the polymer, and R is the gas constant. The Vyazovkin and Sbirrazzuoli method and Hoffman–Lauritzen theory have been widely used in recent literature to calculate U^* and K_g.[51–54]

RESULTS AND DISCUSSION

Nonisothermal crystallization

The nonisothermal crystallization MDSC traces (nonreversing curves) of linear m-PEs at low and high R values (2 and 20°C/min) are shown in Figure 1(a,b). The m-PE crystallization exotherms were fairly similar. They showed a distinct high-temperature peak followed by a minor broad long tail. A primary crystallization was observed at high temperatures, and a secondary crystallization was observed at low temperatures. The different parameters obtained from Figure 1 are listed in Table II. These parameters include: T_o, which is the temperature at the intersection of the tangents of the baseline and the high-temperature side of the exotherm; the peak crystallization temperature (T_c^{peak}); the enthalpy of crystallization (ΔH_c), and X_c. These parameters were obtained at different R's in the range 2–20°C/min.

At low R's (2°C/min), T_o and T_c^{peak} were in the range 124–125 and 120–121°C, respectively. On the other hand, at high R's (20°C/min), T_o and T_c^{peak} were in the range 120–122 and 116–118°C, respectively. So, both T_o and T_c^{peak} shifted to lower values at high R's. However, R had a weaker influence on T_o in comparison with its influence on T_c^{peak}. At both

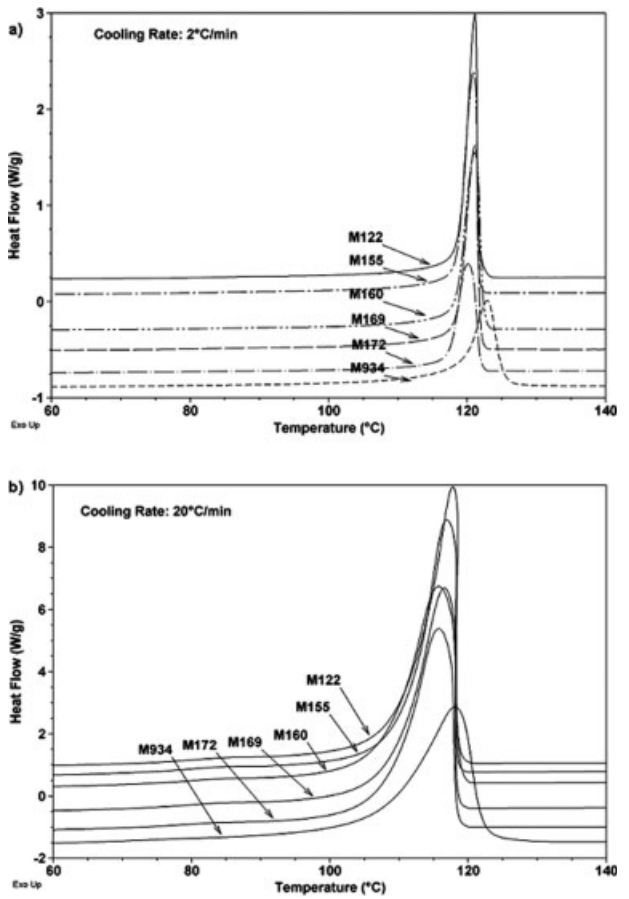

Figure 1 Differential scanning calorimetry nonisothermal crystallization exotherms of metallocene high-density polyethylenes (m-HDPEs) with R's of (a) 2 and (b) 20°C/min.

TABLE II
Thermodynamic Properties of the Linear m-PEs

R (°C/min)	Resin	T_o (°C)	T_c^{peak} (°C)	ΔH_c (J/g)	X_c (%)
2	M122	124.2	121.11	184.6	63.64
	M155	124.0	120.93	172.3	59.72
	M160	124.0	120.98	169.6	58.49
	M169	124.0	121.14	170.1	58.65
	M172	124.1	120.15	163.3	56.31
	M934	125.2	122.89	128.9	44.44
5	M122	122.50	120.70	179.9	62.05
	M155	120.8	116.85	168.1	57.97
	M160	123.1	119.29	163.7	56.44
	M169	121.2	116.68	160.76	55.43
	M172	122.6	119.57	162.3	55.95
	M934	124.1	121.46	124.1	42.78
10	M122	121.5	119.31	168.8	58.22
	M155	121.0	118.37	162.3	55.96
	M160	121.5	117.56	154.3	53.22
	M169	121.5	117.91	153.2	52.81
	M172	121.0	118.03	150.6	51.94
	M934	123.1	120.02	116.2	40.08
20	M122	121.0	117.8	172.0	59.31
	M155	120.0	116.95	164.2	56.63
	M160	121.0	115.75	156.2	53.88
	M169	120.5	116.61	158.1	54.51
	M172	120.5	115.76	147.2	50.76
	M934	122.0	118.12	117.9	40.66

low and high R's, X_c showed a significant drop ($\sim$ 30%) when M_w was increased from 122 to 934 kg/mol. In addition, the drop in crystallinity as a result of increased R was less than 10%.

The crystallization exotherm data obtained at 2 and 20°C/min are shown in Figure 2(a,b). X_T was calculated with eq. (3). The results for all samples and at all rates are given in Table II. X_T was then converted into X_t by transformation of the temperature axis to the time analogue with eq. (4). X_t versus t is plotted in Figure 3(a,b). Initially, an attempt was made to fit the whole data of m-PEs with the Avrami analysis, as shown in Figure 4(a,b). Figure 4(a,b) represents the Avrami plots of all m-PEs at 2 and 20°C/min, respectively. Data at other rates are not shown here; however, the extracted parameters are displayed in Table III. It was clear that the observed variations in the n values were due to the poor fit of the Avrami equation for the whole range, as reflected in the regression coefficient. However, this was also observed in all of the previous publications that used the Avrami equation to fit the whole range of data. Therefore, it is a problem of the model used. On the other hand, the other method of data

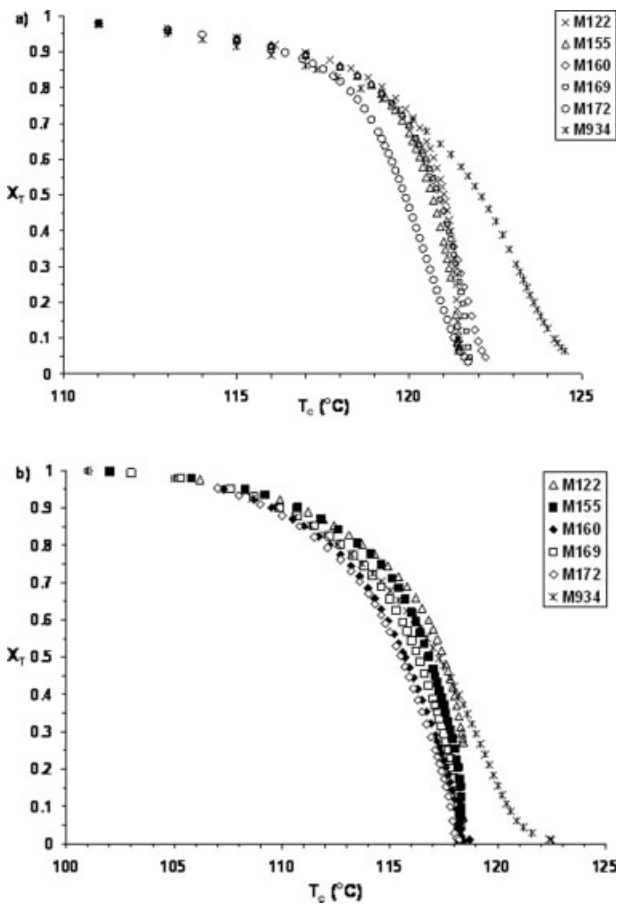

Figure 2 Development of X_T with T_c for m-HDPEs with R's of (a) 2 and (b) 20°C/min.

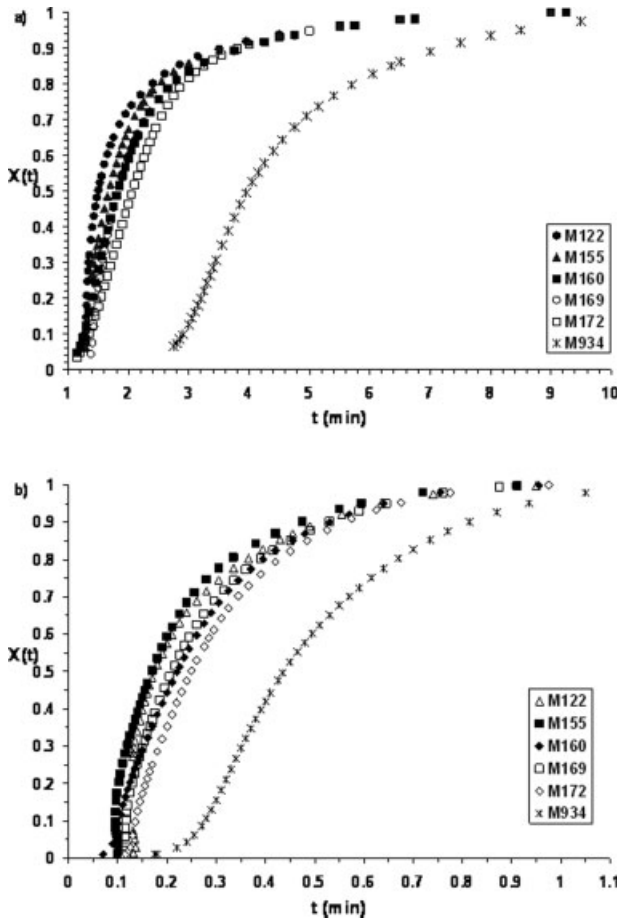

Figure 3 Development of the relative degree of crystallinity [$X(t)$] with t for m-HDPEs with R's of (a) 2 and (b) 20°C/min.

analysis that uses the activation energy (Hoffman–Lauritzen theory) results in much better fitting because the method assumes the activation energy to be temperature dependent.

All m-PEs showed two linear parts. At low R's (at 2 and 5°C/min), the second linear part approached a plateau, whereas at high R's (10 and 20°C/min), the linear portion had a more positive slope. All m-PEs were linear molecules with very similar MWDs (2–3). Hence, the only explanation for the observation of the second linear part was through the primary and secondary crystallization approach suggested by Wunderlich.[55] The mechanism of secondary crystallization was suggested to be either a crystal perfection process or a crystal thickness growth.[55] Similar deviations in the Avrami plots were reported by several authors in similar crystallization studies. For example, see the results of Jiao et al. [Fig. 6(a) of ref. 24]; Janimak and Stevens [Fig. 5 of ref. 30] for m-LLDPE, and Liu et al. [Fig. 7 of ref. 48] for copolyterephthalamide. Janimak and Stevens[30] used a single line to fit the whole set of data, applying the least squares method.

The values of n, k_t, k_R, and the coefficient of determination (r^2) are listed in Table III. At a R of 2°C/min, n increased from 2.5 to 3.6 when the M_w was increased from 122 to 934 kg/mol. The average value of n was 3. These values were in agreement with previous literature reports on linear PE that suggested spherulitic growth with the n values in the range of 3–4.[56,57] At high rates (20°C/min), n was in the range 1.6–2.6 with an average of 2. The value of n was usually an integer between 1 and 4 for different crystallization mechanisms and a fraction for secondary crystallization.[57,58] Hence, n had a weak R dependency, which suggested that the type of crystal was likely independent of R. The fact that the average values of n were either 2 or 3 suggested that there was instantaneous nucleation.[59] The main reason for having fractional n values is the data fitting, which was evident in the regression coefficient (see Table III). For other reasons that can result in fractional n values, see the review article by Piorkowska et al.[59] However, the primary crystallization rate parameters (k_{t1} and k_{R1}), given in Table III, decreased with increasing M_w at low R's (2 and

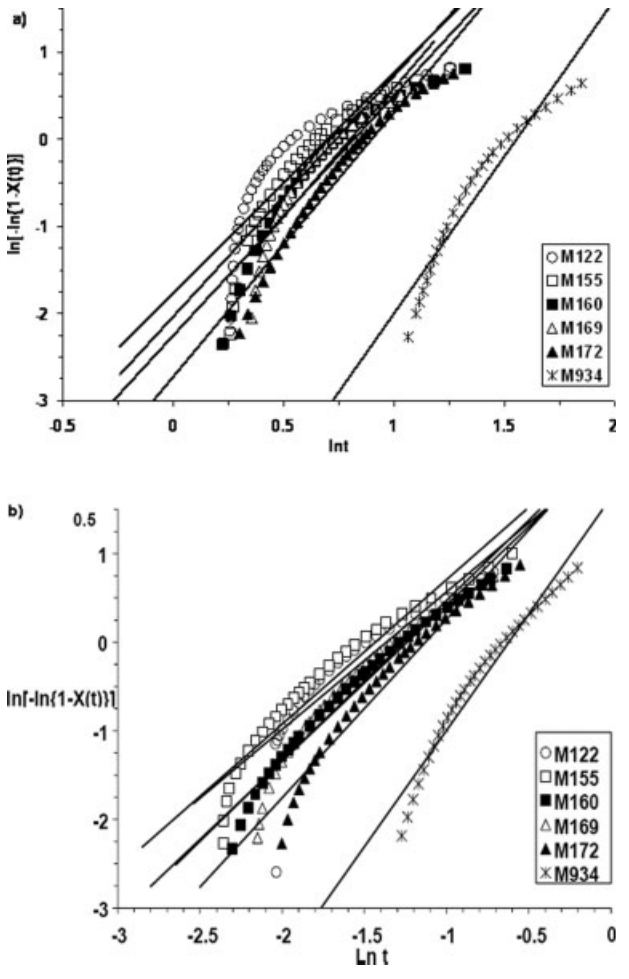

Figure 4 Avrami plots for m-HDPEs with R's of (a) 2 and (b) 20°C/min.

TABLE III
Avrami Parameters for the Linear m-PEs

		Primary crystallization			
R (°C/min)	Resin	n_1	k_{t1}	k_{R1}	r^2
2	M122	2.53	0.172	0.415	0.74
	M155	2.76	0.131	0.362	0.84
	M160	2.76	0.106	0.325	0.89
	M169	2.96	0.094	0.307	0.88
	M172	3.00	0.066	0.257	0.96
	M934	3.61	0.004	0.061	0.93
5	M122	1.64	2.317	1.522	0.77
	M155	2.19	1.022	1.011	0.99
	M160	2.45	1.025	1.012	0.94
	M169	2.45	0.757	0.87	0.97
	M934	3.8	0.051	0.226	0.93
10	M122	1.83	6.945	1.214	0.81
	M155	1.9	6.199	1.2	0.93
	M160	1.99	4.152	1.153	0.97
	M169	1.98	4.848	1.171	0.96
	M172	2.06	4.622	1.165	0.96
	M934	3.78	0.604	0.951	0.94
20	M122	1.55	8.341	1.112	0.79
	M155	1.63	10.35	1.124	0.92
	M160	1.77	8.925	1.116	0.97
	M169	1.81	9.808	1.121	0.94
	M172	2.02	9.734	1.121	0.96
	M934	2.63	5.111	1.085	0.96

5°C/min). The rate constant was sensitive to both M_w and R. However, at high rates (10 and 20°C/min), k_{R1} was independent of both M_w and R and approached a value of 1.1, as shown in Table III. The M_w dependency of k_{R1} could be fitted by an Arrhenius-type relationship ($k_{R1} = k_{Ro}e^{281}/M_w$, where k_{Ro} is a rate-dependent constant). The values of the constants were rate dependent. At 2°C/min, $k_{R1} = 0.0489e^{289}/M_w$ ($r^2 = 0.958$), whereas at 5°C/min, $k_{R1} = 0.1725e^{273}/M_w$ ($r^2 = 0.966$). The fact that the exponential power was approximately the same, within experimental errors, suggested that the decrease in k_{R1} due to the increase in M_w was an activated state process and the constant (273–289) was related to the activation energy of the primary crystallization. M_w was in kilograms per mole. In addition, the preexponential constant was rate dependent, which is the case in Arrhenius-type relationships. In general, the M_w dependency of k_R was similar to the temperature dependency of viscosity.

Furthermore, a kinetic model proposed by Mo[48] was used [see eq. (7)]. Plots of ln R versus ln t for all of the linear m-PE samples are shown in Figure 5(a,b) for M122 and M934. Plots for other samples are not shown here; however, the Mo parameters for all of the samples are given in Table IV. From these plots, values of α and $F(T)$ were obtained at different crystallinities in the range 20–80%. All plots were linear, as predicted by eq. (7). $F(T)$ increased systematically with the increase in percentage crystallinity. In general, the higher the M_w was, the higher was

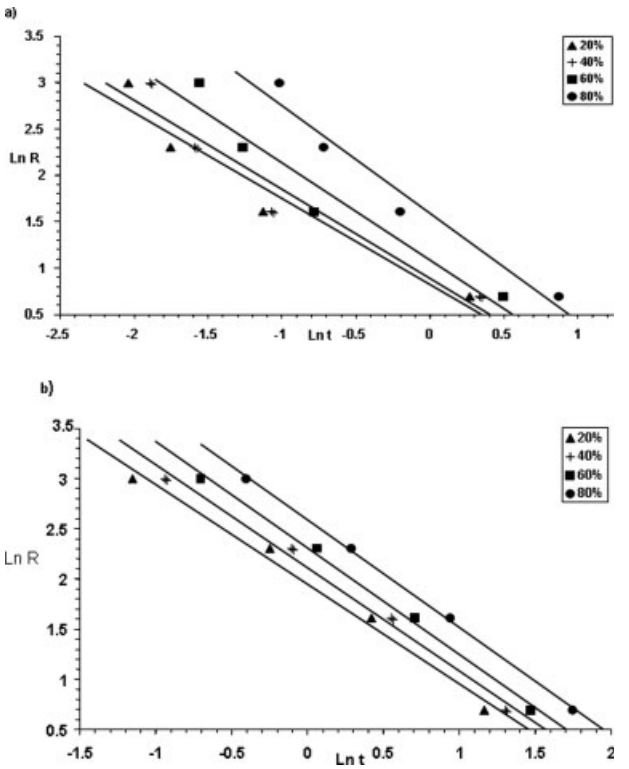

Figure 5 Plots of ln R versus ln t at each given relative crystallization: (a) M122 and (b) M934,

the value of $F(T)$, which suggested an increased difficulty of polymer crystallization. This observation was valid at all levels of crystallization. These results were in agreement with the previous observations on k_{R1} obtained through the Avrami method. So, both the modified Avrami and Mo methods of anal-

TABLE IV
Values of the Mo Parameters, α and $F(T)$, at a Fixed Value of the Relative Degree of Crystallinity [$X(t)$] for All of the Samples

		$X(t)$ (%)			
Resin	Variable	20	40	60	80
M122	α	0.927	0.961	1.048	1.160
	$F(T)$	2.276	2.431	2.963	4.907
	r^2	0.937	0.927	0.934	0.957
M155	α	0.856	0.909	0.979	1.078
	$F(T)$	2.602	3.178	3.96	5.619
	r^2	0.991	0.981	0.980	0.986
M160	α	0.932	1.032	1.112	1.171
	$F(T)$	2.78	3.381	4.310	6.339
	r^2	0.997	0.998	0.998	0.997
M169	α	0.903	0.964	1.035	1.124
	$F(T)$	2.915	3.573	4.491	6.453
	r^2	0.988	0.980	0.980	0.989
M172	α	0.976	1.026	1.085	1.166
	$F(T)$	2.766	3.452	4.376	6.288
	r^2	0.974	0.970	0.971	0.975
M934	α	0.993	1.027	1.060	1.071
	$F(T)$	7	8.238	10.04	13.3
	r^2	0.987	0.992	0.996	1.00

ysis agreed in suggesting an increased difficulty of crystallization with increased M_w.

The Vyazovkin and Sbirrazzuoli[49] method of analysis [eq. (9)], which is based on Hoffman–Lauritzen theory for secondary crystallization,[50] was used. Samples M155 and M934 were taken as examples of low- and high-M_w resins. For linear PE, 416.2 and 153.15 K were used for T_m^o and T_g, respectively.[46] Values of activation energy (E) at different temperatures were obtained with eq. (8). Then, eq. (9) was rewritten in the following format:

$$[\mathbf{E}] = U^*[\mathbf{Z}] + K_g[\mathbf{Y}] \tag{10}$$

where [**E**] is the matrix of activation energy data, [**Z**] and [**Y**] are the matrices of the $\left[\frac{T^2}{(T-T_\infty)^2}\right]$ and $\left[R\frac{(T_m^o)^2-T^2-T_m^oT}{(T_m^o-T)^2T}\right]$ sets, respectively. MatLab software was used for the solution of the previous nonlinear equation. Optimum values of U^* and K_g that fit eq. (10) were obtained and are plotted along with the experimental data in Figure 6. Values of U^* were calculated as 11.8 and 240.7 kJ/mol for M934 and M152, respectively. However, K_g was 95.0 and 225.0 for M934 and M152, respectively. The increase in the kinetic parameter K_g due to the increase in M_w may seem to contradict the previous results from Avrami analysis. However, Hoffman–Lauritzen secondary crystallization theory and the Vyazovkin and Sbirrazzuoli[49] method of analysis are different than the Avrami method, which is mainly for the primary crystallization part of the data (linear part of the curve). The decrease in U^* from 240.7 to 11.8 kJ/mol with the increase in M_w from 152 to 934 kg/mol suggested that a high M_w tended to slow the crystallization process. The decrease in U^* was almost 10 times the increase in K_g. Hence, the Avrami, Mo, and Hoffman–Lauritzen theory methods of analysis agreed in suggesting the strong influence of M_w on slowing the overall crystallization process. This decrease was likely due to decreased molecular transport with increased M_w.

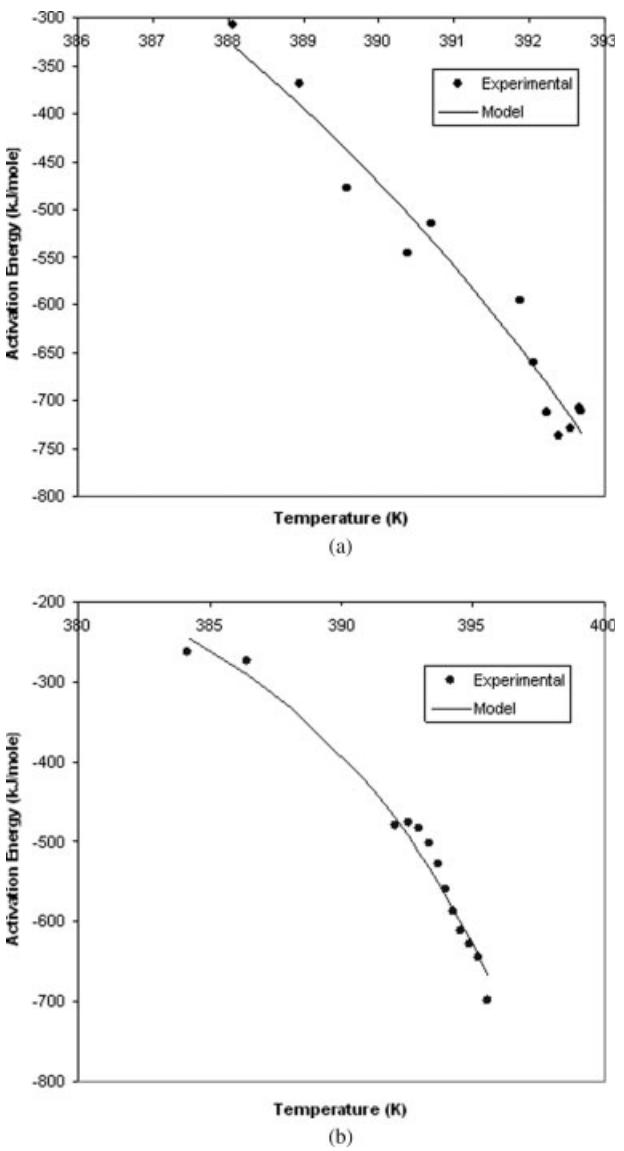

Figure 6 Plots of the activation energy versus the temperature for (a) M152 and (b) M934.

CONCLUSIONS

On the basis of the previous results and discussion, the following was concluded:

1. The nonisothermal crystallization of linear mPEs with M_w's in the range 122–934 kg/mol occurred through primary and secondary crystallization processes.
2. M_w had a weak influence on both T_c^{peak} and T_o. It moved to a lower temperature region as M_w is increased.
3. Both T_o and T_c^{peak} shifted to lower values at high R's. However, R had a weaker influence on T_o in comparison with its influence on T_c^{peak}.
4. Both at low and high R's, crystallinity showed a significant drop ($\sim$ 30%) when M_w was increased from 122 to 934 kg/mol. In addition, the drop in crystallinity as a result of increased R was less than 10%.
5. At low R's ($< 10^\circ$C/min), the rate parameters in the modified Avrami (k_R) and Mo [$F(T)$] methods of analysis agreed in suggesting that increased M_w slowed the rate of crystallization. The M_w dependency of k_R followed an Arrhenius-type relation ($k_R = k_{Ro}\, e^{281/M_w}$). However, at higher R's, k_R approached a constant value.
6. For the primary crystallization, the crystallization constant n (calculated with the Avrami analysis modified by Jeziorny) was insensitive

to M_w Values of n depended on R, in agreement with previous literature reports.[56–58] The order parameters obtained by the different methods of analysis (n and α) were independent of M_w, which suggested that the crystal type remained the same in the studied range.

7. The Vyazovkin and Sbirrazzuoli method of analysis, which is based on Hoffman–Lauritzen theory, was also used, and U^* decreased from 240.7 to 11.8 kJ/mol when M_w was increased from 152 to 934 kg/mol. The kinetic parameter K_g increased from 95.0 to 225.0 when M_w was increased from 152 to 934 kg/mol. Therefore, the decrease in the segmental activation energy was more significant than the increase in the kinetic parameter K_g. The results of Hoffman–Lauritzen theory were in agreement with the Avrami and Mo methods of analysis. All methods suggested the strong influence of a high M_w on the slowing of the crystallization process.

The author is thankful to S. E. Wanke of the Chemical and Materials Engineering Department at the University of Alberta (Canada) for providing the samples and molecular mass data. Furthermore, the author acknowledges the support of King Fahd University of Petroleum & Minerals. The author also thanks Ashraful Islam for his help.

References

1. Ozawa, T. Polymer 1971, 12, 150.
2. Jeziorny, A. Polymer 1978, 19, 1142.
3. Jayakannan, M.; Ramakrishnan, S. J Appl Polym Sci 1999, 74, 59.
4. Sajkiewicz, P.; Carpaneto, L.; Wasiak, A. Polymer 2001, 42, 5365.
5. Qui, Z.; Ikehara, T.; Nishi, T. Polymer 2003, 44, 5429.
6. Kao, Y. H.; Phillips, P. J. Polymer 1986, 27, 1669.
7. Phillips, P. J.; Kao, Y. H. Polymer 1986, 27, 1679.
8. Nordmeier, E.; Lanver, U.; Lechner, M. D. Macromolecules 1990, 23, 1072.
9. Sutton, S. J.; Vaughan, A. S.; Bassett, D. C. Polymer 1996, 37, 5735.
10. Wagner, J.; Abu-Iqyas, S.; Monar, K.; Phillips, P. J. Polymer 1999, 40, 4717.
11. Wagner, J.; Phillips, P. J. Polymer 2001, 42, 8999.
12. Mandelkern, L.; Maxfield, J. J Polym Sci Polym Phys Ed 1979, 17, 1913.
13. Strobl, G. R.; Engelke, T.; Maderek, E.; Urban, G. Polymer 1983, 24, 1585.
14. Maderek, E.; Strobl, G. R. Colloid Polym Sci 1983, 261, 471.
15. Alamo, R.; Domszy, R.; Mandelkern, L. J Phys Chem 1984, 88, 6587.
16. Mandelkern, L. Polym J 1985, 17, 337.
17. Usami, T.; Gotoh, Y.; Takayama, S. Macromolecules 1986, 19, 2722.
18. Alamo, R. G.; Mandelkern, L. Macromolecules 1989, 22, 1273.
19. Fatou, J. G.; Marco, C.; Mandelkern, L. Polymer 1990, 31, 1685.
20. Alamo, R. G.; Viers, B. D.; Mandelkern, L. Macromolecules 1993, 26, 5740.
21. Shanks, R. A.; Amarasinghe, G. J Therm Anal Calorim 2000, 59, 471.
22. Zhang, M.; Lynch, D. T.; Wanke, S. E. Polymer 2001, 42, 3067.
23. Rabiej, S.; Goderis, B.; Janicki, J.; Mathot, V. B. F.; Koch, M. H. J.; Groeninckx, G.; Reymaers, H.; Gelan, J.; Wlochowicz, A. Polymer 2004, 45, 8761.
24. Jiao, C.; Wang, Z.; Liang, X.; Hu, Y. Polym Test 2005, 24, 71.
25. Bensason, S.; Minick, J.; Moet, A.; Chum, S.; Hiltner, A.; Baer, E. J Polym Sci Part B: Polym Phys 1996, 34, 1301.
26. Voigt-Martin, I. G.; Alamo, R.; Mandelkern, L. J Polym Sci Part B: Polym Phys 1986, 24, 1283.
27. Keating, M. Y.; Lee, I. H. J Macromol Sci Phys 1999, 38, 379.
28. Starck, P.; Lehmus, P.; Seppala, V. Polym Eng Sci 1999, 39, 1444.
29. Xu, J.; Xu, X.; Feng, L. Eur Polym J 1999, 36, 685.
30. Janimak, J. J.; Stevens, G. C. Thermochim Acta 1999, 332, 125.
31. Razavi-Nouri, M.; Hay, J. N. Polymer 2001, 42, 8621.
32. Fu, Q.; Chiu, F.; He, T.; Liu, J.; Hsieh, E. T. Macromol Chem Phys 2001, 202, 927.
33. Wang, C.; Chu, M. C.; Lin, T. L.; Lai, S. M.; Shih, H. H. Polymer 2001, 42, 1733.
34. Chiu, F.; Fu, Q.; Peng, Y.; Shih, H. J Polym Sci Part B: Polym Phys 2002, 40, 325.
35. Starck, P.; Löfgren, B. Eur Polym J 2002, 38, 97.
36. Teng, H.; Shi, Y.; Jin, X. J Polym Sci Part B: Polym Phys 2002, 40, 107.
37. Hussein, I. A. Polym Int 2004, 53, 1327.
38. Hameed, T.; Hussein, I. A. Polymer 2002, 43, 6911.
39. Wunderlich, B. In Thermal Characterization of Polymeric Materials, 2nd ed.; Turi, E. A., Ed.; Academic: New York, 1997; Vol. 1.
40. Schawe, J. E. K. Thermochim Acta 1995, 260, 1.
41. Avrami, M. J Chem Phys 1939, 7, 1103.
42. Avrami, M. J Chem Phys 1940, 8, 212.
43. Avrami, M. J Chem Phys 1941, 9, 177.
44. Ziabbicki, A. Colloid Polym Sci 1974, 6, 252.
45. Ziabbicki, A. Appl Polym Symp 1967, 6, 1.
46. Wunderlich, B. Macromolecular Physics; Academic: New York, 1976; Vol. 2, p 147.
47. Tanem, B. S.; Stori, A. Polymer 2001, 42, 5389.
48. Liu, T. X.; Mo, Z. S.; Wang, S. E.; Zhang, H. F. Polym Eng Sci 1997, 37, 568.
49. Vyazovkin, S.; Sbirrazzuoli, N. Macromol Rapid Commun 2004, 25, 733.
50. Hoffman, J. D.; Davis, G. T.; Lauritzen, J. I., Jr. In Treatise on Solid State Chemistry; Hannay, N. B., Ed.; Plenum: New York, 1976; Vol. 3, Chapter 7.
51. Achilias, D. S.; Papageorgiou, G. Z.; Karayannidis, G. P. Macromol Chem Phys 2005, 206, 1511.
52. Cai, J.; Li, T.; Han, Y.; Zhuang, Y.; Zhang, X. J Appl Polym Sci 2006, 100, 1479.
53. Vyazovkin, S.; Dranca, I. Macromol Chem Phys 2006, 207, 20.
54. Botines, E.; Puiggali, J. Eur Polym J 2006, 42, 1595.
55. Wunderlich, B. Macromolecular Physics; Academic: New York, 1976; Vol. 2, p 147.
56. Buchdahl, R.; Miller, R. L.; Newman, S. J Polym Sci 1959, 36, 215.
57. Chen, K.; Tang, X.; Shen, J.; Zhou, Y.; Zhang, B. Macromol Mater Eng 2004, 289, 539.
58. Maderek, E.; Strobl, G. R. Colloid Polym Sci 1983, 261, 471.
59. Piorkowsk, E.; Galeski, A.; Haudin, J.-M. Prog Polym Sci 2006, 31, 549.